
Article:
Chen, Zhendong, Ruan, Xuezhong, Liu, Bo et al. (7 more authors) (2019) Component manipulated magnetic anisotropy and damping in Heusler-like compound Co2+xFe1-xAl. Journal of Physics Condensed Matter. 075802. ISSN 1361-648X

https://doi.org/10.1088/1361-648X/aaf682

Component modulated magnetic anisotropy and damping in Heusler-like compound $Co_{2+x}Fe_{1-x}Al$

Zhendong Chen, Bo Liu, Long Yang, Xuezhong Ruan, Cunxu Gao, Yongbing Xu

Abstract:

The component dependence of the magnetocrystalline anisotropy and the damping has been investigated in epitaxial Heusler-like compound $Co_{2+x}Fe_{1-x}Al$ grown by molecular beam epitaxy with x=-0.4, -0.2, 0, 0.2, and 0.4. All the samples show a component tunable four-fold magnetocrystalline anisotropy with the easy axis along [110] orientation for different samples. Furthermore, the component dependence of the damping coefficient has been studied via time resolved magneto-optic Kerr effect measurements (TR-MOKE). The measurement results reveal that the minimum of damping is obtained for the sample with x=-0.2. This work provides a new approach to modulate the magnetic dynamic properties of Heusler alloy Co_2FeAl by adjusting the proportion of Co and Fe.

Introduction:

In recent decades, spintronic devices for example magnetic random access memory (MRAM) have attracted a lot of interests because of their advantage of high density, low power consumption and non-volatile properties[1]. It is believed widely that the spintronic device is an alternative of the new generation of electric device. Current induced magnetization switch (CIMS) is studied extensively as a key technique for writing message into spintronic devices[2]. It has been reported that the current density j_C required for CIMS is proportional to Gilbert damping constant α[3]. Thus the damping constant of many spintronic materials has been widely investigated, such as FeNi, FeCo and CoFeB[4]-[9]. In variety of spintronic materials, Heusler compound Co_2FeAl (CFA) has caught much attention because of its half-metallic property and low damping[10][11][12]. In past years, the damping of CFA was reported to be as low as 0.001 but had a large scatter varying from 0.001 to 0.04 caused by different sample growth techniques and substrates[11]-[15]. In order to optimize the magnetic dynamic properties of CFA films, variety of parameters have been modulated such as annealing temperature, thickness and doping components[16]-[20]. There is a well-known theory which link internal damping constant to the density of state (DOS) near the Fermi level. The theory demonstrate that the damping constant is proportional to the DOS, which can be described as $\alpha \propto \xi^2 D_F$, where α is the damping constant, ξ is the spin-orbit coupling coefficient and D_F is the DOS near the Fermi level[21][11]. It provides an theoretical support to modify the damping constant of CFA by adjusting the components. While modifying the components in CFA films, people usually use quaternary systems, such as, $Co_2Fe_{1-x}Mn_xAl$, $Co_2Fe_{1-x}Cr_xAl$, $Co_2FeAl_{1-x}Si_x$, and $Co_2FeAl_{1-x}Ge_x$ to contrast with CFA because these systems have the same full-Heusler-like crystalline texture[19][20]. In this work

we report the modulation of magnetic dynamic properties in a new system $Co_{2+x}Fe_{1-x}Al$ by adjusting x from -0.4 to 0.4, in which no new element is brought in.

It is known that the magnetization dynamics can be well described phenomenologically by the Landau-Lifshitz-Gilbert (LLG) equation: $\frac{dm}{dt} = -\gamma m \times H_{eff} + \alpha m \times \frac{dm}{dt}$, where m, H_{eff}, γ and α are the unit vector of magnetization, the effective magnetic field, the gyromagnetic ratio and the Gilbert damping constant, respectively. There are two measurement methods used for investigating the magnetic dynamics of spintronic materials: ferromagnetic resonance (FMR) and time resolved magneto-optic Kerr effect (TR-MOKE)[9][15]. FMR is a traditional measurement for characterizing the magnetic anisotropy and damping of ferromagnetic materials. However, this measurement is limited by the modulation range of the microwave frequency and external fields. In comparison, TR-MOKE, which can observe the procession of magnetization directly, is an effective method to measure the damping constant. In this work we use FMR to measure the magnetic anisotropy of the epitaxial $Co_{2+x}Fe_{1-x}Al$ films grown on MgO (001) substrates. And then TR-MOKE method is used to characterize the damping of each sample. The dependence of the anisotropy and the damping on the adjusting component ratio x is obtained. This work could provide a new approach to modulate the magnetic dynamics of CFA.

Experiment: The epitaxial growth of $Co_{2+x}Fe_{1-x}Al$ films were implemented in a custom-built MBE system equipped with solid-source effusion cells for Co, Fe and Al. Nucleation and growth were monitored in situ by reflection high-energy electron diffraction (RHEED). Prior to growth, the MgO(001) substrate was chemically cleaned, desorbed water, and then transferred into the deposition chamber. The substrate was further thermally cleaned to remove the surface oxide, and 9 nm thick $Co_{2+x}Fe_{1-x}Al$ films were then deposited at a substrate temperature of 200 ^{o}C with x=-0.4, -0.2, 0, 0.2, and 0.4. Quartz microbalance was employed in situ to obtain the chemical composition and thickness of the films. Static magnetic properties of the samples including the remnant magnetization curves (RMC) and hysteresis loops were recorded at room temperature by vibrating sample magnetometry (VSM). For these RMC measurements, remnant magnetization was measured with the films rotated around their normal axis in a step of 5^{o}. In every step, the CFA films were first magnetized in-plane at a saturate field of 3000 Oe followed by removing the field and then recording data. Then the hysteresis loops were measured along the easy axis where the maximum remnant magnetization occur and the hard axis where the minimum remnant magnetization occur for each sample, respectively. The magnetic anisotropy was investigated by in-plane rotating FMR with the microwave frequency of 9.78 GHz. Before the measurements began, the films had been set as the external field along the [100] orientation of the MgO substrates. And then the measurements were implemented at every 15^{o} as the samples were rotated. Finally, the damping constant were obtained by polar TR-MOKE. The femtosecond pulse train generated by a regenerative amplifier Ti: sapphire laser with a pulse duration of 50 fs and a repetition of 1kHz was divided into pump and probe pulse beam. The fluence, wavelength and spot diameter of the pump pulse beam are 5.10

mJ/cm^2, 800 nm and 500 μm, respectively. And correspondingly, these parameters of the probe pulse beam are 40.82 μJ/cm^2, 400 nm and 250 μm, respectively. The external field was applied in the [001]/[110] plane and with 30^o deviating from the in-plane [110] orientation, and with the intensity of 1330 Oe, 2592 Oe, 3865 Oe, 5122 Oe, 6351 Oe, 7534 Oe and 8830 Oe.

Results and discussion:

Fig. 1(a) shows the stationary RHEED patterns of the MgO(001) and $Co_{2+x}Fe_{1-x}Al$ surface along MgO[001] orientation with the x=-0.4, 0, and 0.4. The patterns evidence a well epitaxial films. It is obviously exhibited that the crystalline structures of all the $Co_{2+x}Fe_{1-x}Al$ samples are in a same type with x varying from -0.4 to 0.4. It has been reported wildly that the structure of Co_2FeAl follows the $Fm\bar{3}m$ space group as all the full-Heusler compounds[12][16][17]. Thus it is suggested that all the samples with x varying from -0.4 to 0.4 have the same Heusler-like cubic crystalline structure. The RHEED patterns also display that the growth orientation are as $Co_{2+x}Fe_{1-x}Al(001)[110]//MgO(001)[100]$ for each x (Fig. 1(b)), which is the same as the status of Co_2FeAl grown on MgO(001) substrates.

In order to investigate the static magnetic properties of the samples, VSM measurements have been performed to obtain the RMC and hysteresis loops. In Fig. 1(c) and 1(d) it is clearly revealed that all the $Co_{2+x}Fe_{1-x}Al$ films show an obvious four-fold magnetic anisotropy superimposed with a subordinate uniaxial anisotropy. The easy axis of the four-fold magnetic symmetry is along $Co_{2+x}Fe_{1-x}Al[110]$ orientation. The four-fold symmetry is believed to originate from the intrinsic magnetocrystalline anisotropy of the cubic $Co_{2+x}Fe_{1-x}Al$ lattice. While the weak uniaxial symmetry is induced by the lattice stress derived from the mismatch between the substrate and the films. It is suggested that the component modulation does not influence the magnetic symmetry of the samples on account of the consistent lattice symmetry. In addition, the relationship between saturation magnetization and component ratio x is exhibited in Fig. 1(e). it is revealed that the saturated magnetization reduces with the increase of Co component. This trend is not coincident with the Slater-Pauling principle, which predicts that the saturated magnetization is positive linear with the valence electron number per formula in Heusler compounds[22]. It may be caused by the disorder of the lattice configuration driven by component modulation.

For quantifying the magnetic anisotropy with varying component ratio x, in-plane rotatable FMR was used to measure the resonance spectra at different orientation of the samples. Fig. 2(a) contains a sketch of the FMR coordinate system where φ and φ_H are the azimuthal angle, and θ and θ_H are the polar angles of the magnetization M and the external field H, respectively. The measurement results given in Fig. 2(b) also shows a distinct four-fold spatial symmetry superimposed with a subordinate uniaxial symmetry for the resonant peak in all the samples with different component. It reveals an identical conclusion with the static measurements on the magnetic symmetry. The spatial symmetry of resonant peak can be described by the Smit-Beljers equation[23],

$$\left(\frac{\omega}{\gamma}\right)^2 = \frac{(F_{\theta\theta}F_{\varphi\varphi} - F_{\theta\varphi}^2)}{M_s^2 \sin^2\theta}, \tag{1}$$

where ω, γ, Ms are the microwave circular frequency, the gyromagnetic ratio and the saturated magnetization, respectively. F is the free energy density which is formulated as following for films with four-fold symmetry[23]:

$$\begin{aligned} F = &-M_s H_r[\sin\theta\sin\theta_H\cos(\varphi-\varphi_H) + \cos\theta\cos\theta_H] - (2\pi M_s^2 - K_{2\perp})\sin^2\theta \\ &+ K_{2\parallel}\sin^2\theta\cos^2(\varphi-\varphi_u) - \frac{1}{2}K_{4\perp}\cos^4\theta - \frac{1}{8}K_{4\parallel}(3+\cos4\varphi)\sin^4\theta, \end{aligned} \tag{2}$$

where Hr is the resonance field, $K_{2\perp}$ and $K_{2\parallel}$ are the out-of-plane and in-plane uniaxial anisotropy constant, $K_{4\perp}$ and $K_{4\parallel}$ are the out-of-plane and in-plane four-fold anisotropy constant, and φ_u is the azimuthal angle between the easy axis of the uniaxial anisotropy and the CFA[100]. From Eqs. (1) and Eqs. (2) the relationship for ω, H_r and φ can be obtained as following:

$$\begin{aligned} \left(\frac{\omega}{\gamma}\right)^2 = &\left[H_r\cos(\theta-\theta_H) + \left(\frac{K_{4\perp}}{M_s} + \frac{K_{4\parallel}}{2M_s}\right)\cos4\theta \right. \\ &\left. + \left(-4\pi M_s + \frac{2K_{2\perp}}{M_s} + \frac{2K_{2\parallel}}{M_s} + \frac{K_{4\perp}}{M_s} - \frac{K_{4\parallel}}{2M_s}\right)\cos2\theta\right] \\ &\times\left[H_r\cos(\theta-\theta_H) - \frac{2K_{2\parallel}}{M_s} - \frac{2K_{4\parallel}}{M_s} + \left(\frac{2K_{4\perp}}{M_s} + \frac{K_{4\parallel}}{M_s}\right)\cos^4\theta \right. \\ &\left. + \left(-4\pi M_s + \frac{2K_{2\perp}}{M_s} + \frac{2K_{2\parallel}}{M_s} + \frac{K_{4\parallel}}{M_s}\right)\cos^2\theta\right], \end{aligned} \tag{3}$$

In view of $\theta = \theta_H = 0$, and let $K_{4\perp} \approx 0$, $K_{2\perp} \approx 0$, the equation can be simplified as:

$$\begin{aligned} \left(\frac{\omega}{\gamma}\right)^2 = &\left[H_r\cos(\varphi-\varphi_H) + 4\pi M_s - \frac{2K_2}{M_s}\cos^2(\varphi-\varphi_u) + \frac{K_4}{2M_s}(3+\cos4\varphi)\right] \\ &\times\left[H_r\cos(\varphi-\varphi_H) - \frac{2K_2}{M_s}\cos2(\varphi-\varphi_u) + \frac{2K_4}{M_s}\cos4\varphi\right] \end{aligned} \tag{4}$$

When the measurements were started, 0° was set along [110] orientation of $Co_{2+x}Fe_{1-x}Al$ films. The red dotted lines in Fig. 2(a) shows the fitting results of resonant fields as a function of the magnetization orientation under saturated magnetized approximation. The dependence of quantitative anisotropic coefficients K_2 and K_4 on component ratio x is given out in Fig. 2(b). It is clearly demonstrated that the four-fold symmetry anisotropic coefficient K_4 is of a dominating status with changing x, as well as one order of magnitude larger than K_2. This result suggests that the intrinsic magnetocrystalline anisotropy has already covered up the interface-induced uniaxial anisotropy for 9 nm $Co_{2+x}Fe_{1-x}Al$ films. The maximum of K_4 appears at x=0 and is equal to 0.81×10^5 erg/cc, which suggest that Co_2FeAl has the largest four-fold anisotropy among the samples with different constituent.

The damping-constituent dependence is observed via polar TR-MOKE measurements. The geometrical configuration of the measurement is given in Fig. 3(a). The damped oscillations of magnetization excited by the pump laser are clearly recorded for each films. Fig. 3(b) shows the

TR-MOKE signal of the films with x=0 under the magnetic fields from 1330 Oe to 8830 Oe. By solving the LLG equation it can be demonstrated that the oscillation curve can be fitted by a damped-harmonic function superimposed with an exponential-decaying background[18],

$$y = ae^{-\nu t} + be^{-\frac{t}{\tau}}\sin(2\pi f t + \varphi). \quad (5)$$

Here, a is the background magnitudes and ν is the decay ratio of the background signal, b, τ, f, and φ are the amplitude, spin relaxation time, frequency and phase of magnetization precession, respectively. The red lines are the fit results by the single frequency oscillation function above, suggesting that the optically excited magnetization precession is a uniform mode. The same fitting method was used to manage the Kerr signal of all the films. Fig. 3(c) shows the data and the fitting results of the films with variable x under the external field of 8830 Oe. It is visible that the relaxing process of precession is much lower for the films with $x \leq 0$ compared with which $x > 0$.

By fitting the TR-MOKE signal with Eq. (5), the *f-H* dispersion dependence and spin relaxation time τ with varying H is obtained for every films as Fig. 4(a) and Fig. 4(b) exhibits. The red lines in Fig. 4(a) are the fitting results of the *f-H* relationship obtained by Eqs. (3). The equilibrium position of M_s is determined by the minimum of F by using the conditions $\frac{\partial F}{\partial \theta} = 0$ and $\frac{\partial F}{\partial \varphi} = 0$. It is obvious that the *f-H* relationship is almost the same with different components, which suggest that the in-plane anisotropy is not contributing compared with the large external fields and the demagnetizing fields. From the LLG equation we can obtain the relationship between spin relaxation time τ and the Gilbert damping constant α as the following equation[24],

$$\frac{1}{\tau} = \frac{\alpha\gamma}{2M_s}\left(F_{\theta\theta} + \frac{F_{\varphi\varphi}}{\sin^2\theta}\right). \quad (6)$$

Thus the effective damping constant can be calculated by Eqs. (6) and (2) under the view of the geometric status of $\varphi = \varphi_H = \varphi_u = 45^o$ and eliding perpendicular anisotropy. Fig. 4(c) provides the magnetic field dependence of effective damping constant for the samples. It is known that the effective damping approximate the intrinsic damping when the external magnetic field is high enough[15][25]. So we extract all the τ and α under the maximum field of 8830 Oe and plot them as a function as component ratio x in Fig. 4(d). It could be pointed out that the maximum τ and the minimum α both appear at x=-0.2 rather than 0, which means that $Co_{1.8}Fe_{1.2}Al$ has the longest spin relaxation time and the lowest damping. The minimum α is 0.0065, which is smaller than conventional spintronical materials like FeNi[4][5]. In view of the relationship between the damping constant and the DOS in the theory, the lowest damping could suggest lower DOS near the Fermi Level. The damping constant of the Co_2FeAl sample is measured as 0.0078. It is larger than the minimum value obtained by previous work but comparable with the results of other reports[11], [13]-[15].

Conclusion:

Epitaxial Heusler-like compound $Co_{2+x}Fe_{1-x}Al$ films have been prepared via molecular beam epitaxy (MBE) with the x varying from -0.4 to 0.4. In-situ RHEED patterns suggest that the crystalline orientation of the samples follows $Co_{2+x}Fe_{1-x}Al(001)[110]//MgO(001)[100]$. The VSM and FMR results show a component tunable four-fold magnetocrystalline anisotropy with the easy axis along [110] orientation. The maximum crystalline anisotropic constant, which is 0.81×105 erg/cc, appears at x=0. Furthermore, TR-MOKE has been used to study the component dependence of the damping constant. The results reveal that the minimum of damping is obtained as 0.0065 at x=-0.2. This work provides a new approach to modulate the magnetic dynamic properties of Heusler alloy Co_2FeAl by adjusting the proportion of Co and Fe.

Reference:

[1] C. Chappert, A. Fert and Van Dau F. Nguyen, *Nature Mater.* **6,** 813 (2007).

[2] M. Nakayama, T. Kai, N. Shimomura, M. Amano, E. Kitagawa, T. Nagase, M. Yoshikawa, T. Kishi, S. Ikegawa, and H. Yoda: J. *Appl. Phys.* 103 (2008) 07A710.

[3] J. C. Slonczewski, *J. Magn. Magn. Mater.* **159**, L1 1996.

[4] S. Mizukami, Y. Ando, and T. Miyazaki: *Jpn. J. Appl. Phys.* 40 (2001) 580.

[5] S. Mizukami, H. Abe1, D. Watanabe, M. Oogane1, Y. Ando, and T. Miyazaki, *Applied Physics Express* 1 (2008) 121301.

[6] X. Guo, L. Xi, Y. Li, X. Han, D. Li, Z. Wang, and Y. Zuo, *Appl. Phys. Lett*. **105**, 072411 (2014).

[7] Conca, A. *et al.* Low spin-wave damping in amorphous CoFeB thin flms. *J. Appl. Phys.* **113,** 213909 (2013).

[8] Conca, A. *et al.* Annealing influence on the Gilbert damping parameter and the exchange constant of CoFeB thin flms. *Appl. Phys. Lett.* **104,** 182407 (2014).

[9] H. Q. Tu, B. Liu, D. W. Huang, X. Z. Ruan, B.You, Z. C. Huang, Y. Zhai, Y. Gao, J. Wang, L. J. Wei, Y.Yuan, Y. B. Xu and J. Du, *Sci. Rep.* 7, 43971 (2017).

[10] H. C. Kandpal, G. H. Fecher and C. Felser, , *J. Phys. D: Appl. Phys.* **40**, 1507 (2007).

[11] S. Mizukami, D. Watanabe, M. Oogane, Y. Ando, Y. Miura, M. Shirai and T. Miyazaki, *J. Appl. Phys.* **105**, 07D306 (2009).

[12] S. Trudel, O. Gaier, J. Hamrle and B. Hillebrands, J. Phys. D: Appl. Phys. **43**, 193001 (2010).

[13] G. Ortiz, M. S. Gabor, T. Petrisor, Jr., F. Boust, F. Issac, C. Tiusan, M. Hehn, and J. F. Bobo, *J. Appl. Phys.* 109, 07D324 (2011).

[14] H. Sukegawa, Z. Wen, K. Kondou, S. Kasai, S. Mitani, and K. Inomata, *Appl. Phys. Lett.* **100**, 182403 (2012).

[15] S. Qiao, S. Nie, J. Zhao, Y. Huo, Y. Wu, and X. Zhang, *Appl. Phys. Lett.* 103, 152402 (2013).

[16] M. S. Gabor, T. Petrisor Jr., C. Tiusan, M. Hehn, and T. Petrisor, *Phys. Rev. B,* **84,** 134413 (2011).

[17] M. Belmeguenai, H. Tuzcuoglu, M. S. Gabor, T. Petrisor, Jr., C. Tiusan, D. Berling, F. Zighem, T. Chauveau, S. M. Cherif, ´ and P. Moch, *Phys. Rev. B* **87**, 184431 (2013).

[18] S. Qiao, S. Nie, J. Zhao, and X. Zhang, *Appl. Phys. Lett.* 105, 172406 (2014).

[19] Y. Sakuraba, S. Kokado, Y. Hirayama, T. Furubayashi, H. Sukegawa, S. Li, Y. K. Takahashi, and K. Hono, *Appl. Phys. Lett.* 104, 172407 (2014).

[20] K. Özdoğan and B. Aktaş, *J. Appl. Phys.* **101**, 073910 (2007).

[21] V. Kambersky, Can. J. Phys. B, **48**，2906 (1970).

[22] Galanakis I, Dederichs P H. Half-metallicity and Slater-Pauling behavior in the ferromagnetic Heusler alloys[M]//Half-metallic Alloys. Springer, Berlin, Heidelberg, 2005: 1-39.

[23] K. Lenz, E. Kosubek, K. Baberschke, and H. Wende, *Phys. Rev. B* **72**, 144411 (2005).

[24] S. Mizukami, Y. Ando and T. Miyazaki *Jpn. J. Appl. Phys.* **40** 580 (2001).

[25] B. Liu, X. Ruan, Z. Wu, H. Tu, J. Du, J. Wu, X. Lu, L. He, R. Zhang, and Y. Xu, Appl. Phys. Lett. 109, 042401 (2016).

Fig. 1

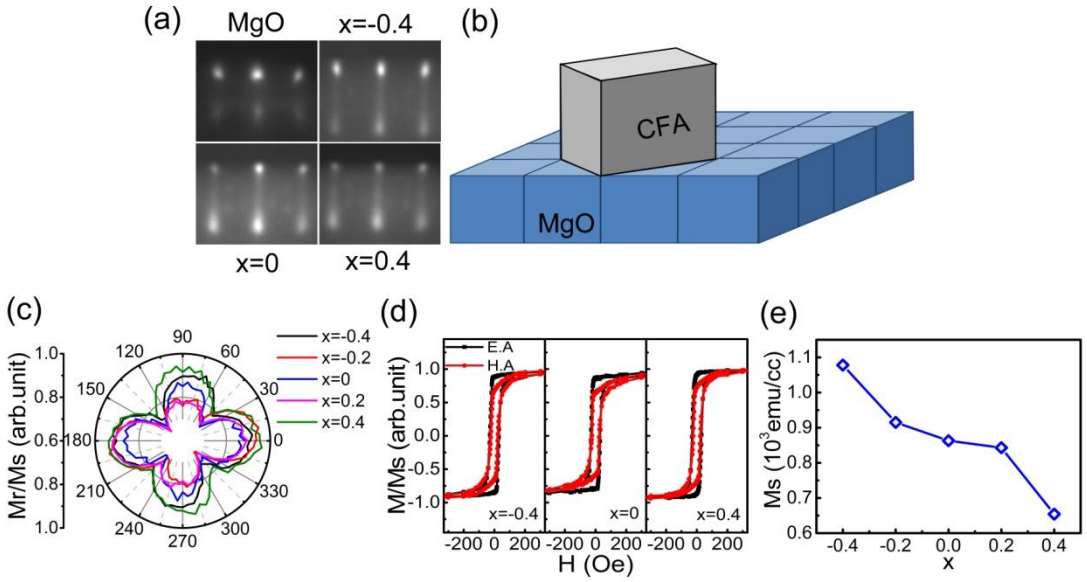

Fig. 1. (a) RHEED patterns of MgO substrate and $Co_{2+x}Fe_{1-x}Al$ films with x=-0.4, 0, 0.4. The orientation of the electron beam is along MgO[100]. (b) Epitaxial crystal orientation relationships between $Co_{2+x}Fe_{1-x}Al$ and MgO(001) substrate. (c) Polar plot of the in-plane angle dependent remanence of CFA films with different thickness. The 0 degree denotes the in-plane $Co_{2+x}Fe_{1-x}Al$ [110] direction. (d) Hysteresis loops of the $Co_{2+x}Fe_{1-x}Al$ films with x=-0.4, x=0, and x=0.4 along the easy axis (E.A.) and the hard axis (H.A.), respectively. (e) Saturation magnetization *vs* component ratio x.

Fig. 2

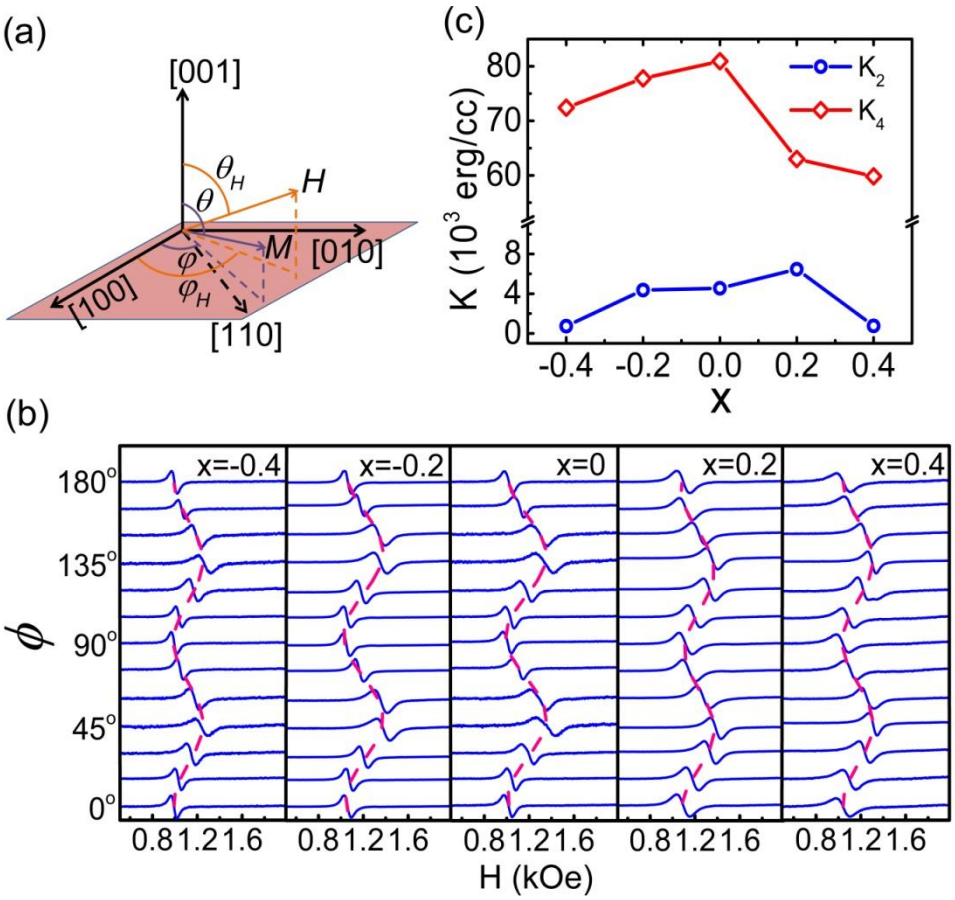

Fig. 2. (a) The sketch of the coordinate system the FMR measurements; (b) FMR spectra of the samples along different orientation. ϕ is the angle between in-plane $\boldsymbol{H}$ and crystal direction [110] of $Co_{2+x}Fe_{1-x}Al$. The red dotted lines are the fitting results of the resonant field-angle dependence. (c) Component dependence of the four-fold anisotropic constant K_4 and uniaxial anisotropic constant K_2.

Fig. 3

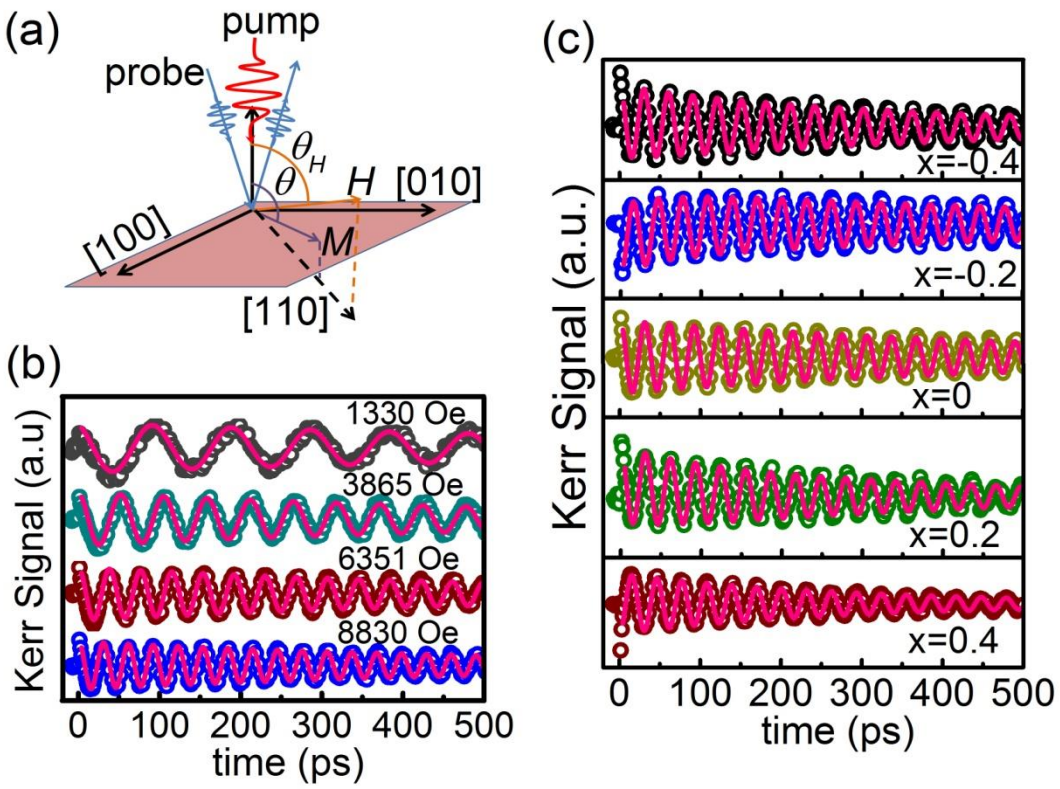

Fig. 3. (a) Geometry diagram of the TR-MOKE measurements. (b) Damping precession signals of Co_2FeAl films under the external fields from 1330 Oe to 8830 Oe. The red lines are the fitting results. (c) Damping precession signals (circles) and fitting results (red lines) of $Co_{2+x}Fe_{1-x}Al$ with x=-0.4, -0.2, 0, 0.2, 0.4 under the external fields of 8830 Oe.

Fig. 4

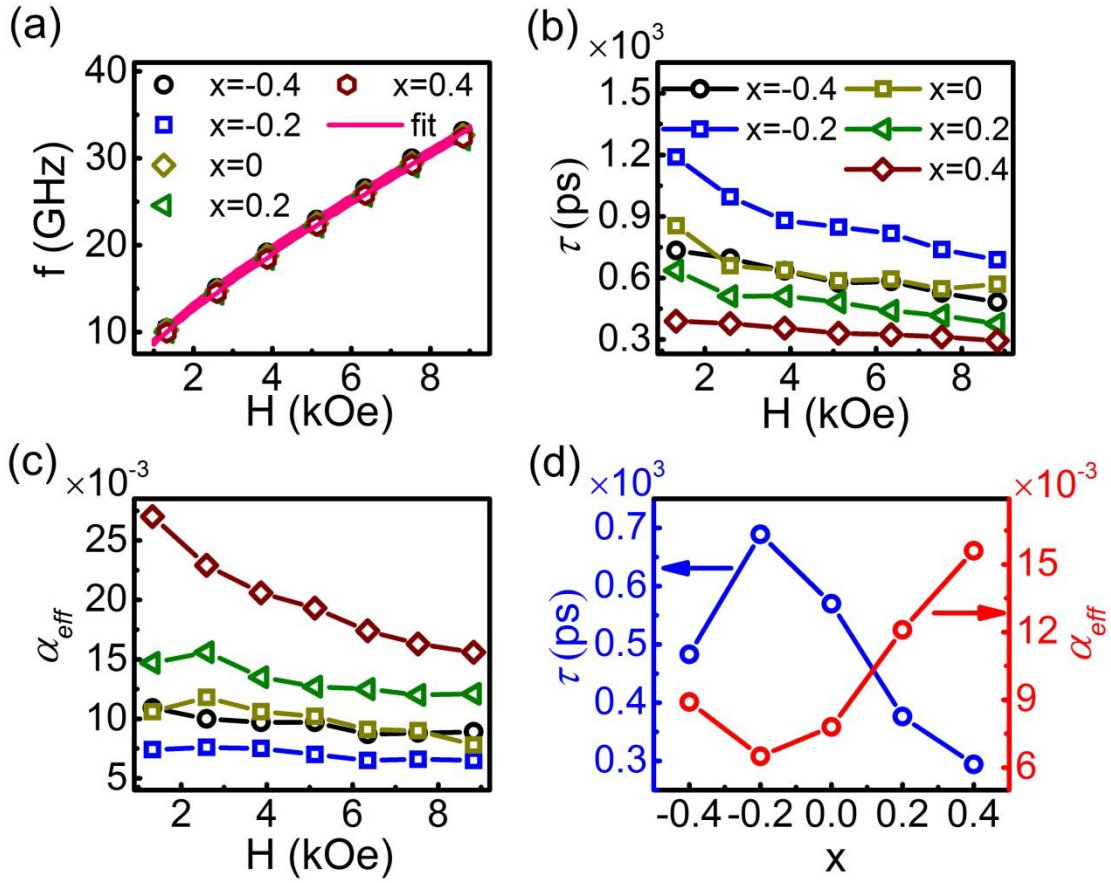

Fig. 4. (a) The frequency-field dependence (dots) and its fitting results (red lines) for the films. (b) spin relaxation time τ as a function of the external field H for $Co_{2+x}Fe_{1-x}Al$ films with different x. (c) Effective damping constant α_{eff} as a function of the external field H for the films. (d) Component dependence of τ (blue square dots and line) and α_{eff} (red circle dots and line) with varying x.